Receptive Field and Neural Networks Representations

Luis Alfredo Avendaño Muñoz. *
School of Computing
University of Leeds
Leeds, United Kingdom
sclaam@leeds.ac.uk

Abstract

In this paper we empirically investigate the effect that the receptive field has on a network's trainability and its one-shot potential. Our results are validated on VGG and ReseNet50 architecture and in CIFAR10 and Tiny ImageNet. We also fine-tune the models to test their real-world application.

1 Introduction

Neural networks have emerged as the standard approach for a wide range of applications, ranging from image recognition [Deng et al., 2009] to natural language processing [Devlin et al., 2019] and speech synthesis [LeCun et al., 2015; van den Oord et al., 2016]. Neural networks owe their expressiveness to the ability to learn hierarchical features and representations form the data that are particularly suited for the task at hand [Goodfellow et al., 2016]. These features are influenced by the highly non-linear.

The reason that make neural networks so good is the features that they learn from the data ([Zhou et al., 2015]), They learning general features in the first layers while in deeper layer they integrate and combine the simpler features and create more complex and detailed features. One aspect that greatly affects these representations, as well as training dynamics is the receptive field of neural networks, yet, its effect on the representations remains not fully understood.

In this paper we systematically explore the relationship that the receptive field has with the representations of neural networks along with the loss landscape these models. We show that if we manipulate the receptive field by changing the kernel size of the first maxpooling layer leaving every other component static we can demonstrate that the models losses generalization capacity as we increase the receptive field. Surprisingly, for high levels of pruning, it turns out that the negative effect on accuracy have an inverse relationship with the receptive field. We show that the receptive fields greatly affects the loss landscape of the models as shown by the Hessian spectra at initialisation.

We empirically validated our results with two different type of models with similar number of parameters (VGG-like and Resnet50) and two different datasets with different image sizes,(CIFAR10 and Tiny imagenet)

Our contributions are:

- We show that the receptive field is linked to the "ruggedness" of the loss landscape of neural networks affecting its trainability and the robustness of its representations to pruning.

*Use footnote for providing further information about author (webpage, alternative address)—*not* for acknowledging funding agencies.

2 Related Work

Previous works have been done in exploring the receptive field in deep convolutional neural networks. Luo et al. [2016] investigate the *Effective Receptive Field* (ERF) of a neural network. ERF is smaller than the theoretical receptive field and grows as the training progresses. They also showed how subsampling and dilation affect the ERF. In Kobayashi and Shouno [2020] the authors find that ResNets have orientation-selective neurons and double opponent colour neurons by investigating the preferred stimulus of the receptive field for a particular neuron. Lastly, [Kim et al., 2023] is the closest work to ours, in which they try to link the receptive field to the accuracy of the model. This work uses different models of the ResNet and WideResNet family and compares their performance and receptive fields. The main problem with this approach is that any change in accuracy might not be directly attributable to the receptive field given the differences in the number of parameters, depth, and width between different models. Thus, our work measures the effect of only modifying the receptive. Furthermore, our work shows the specific effect that modifying the receptive field has on a neural network loss landscape, namely the "ruggedness" of the loss landscape, as well as its performance in a better controlled environment.

3 Experimental results

In this section we empirically investigate the effect that the receptive field has in a network's trainability and prunability. We Statistically validate our results on VGG and ReseNet50 architecture and in CIFAR10 and Tiny ImageNet datasets.

Here I never talked of how I calculated the receptive field, which I used a libary that calculates the gradient projection in a dummy input space with a projected gradient of 1 in the middle of all the fueature maps of the last convolutional layer for the two architectures.

3.1 Experimental settings

We used a custom implementation of the ResNet50 and VGG models with a modified maxpooling layer after the first convolutional layer for manipulating the receptive field. Implementation details are in Section I. The dataset are CIFAR10 and Tiny ImageNet. The training hyperparameters are the following:

- Epochs: 200
- Optimizer: SGD
- Learning rate: 0.0001
- Learning rate schedule: Cosine annealing with $T_{max} = 200$
- Momentum: 0.9
- Weight Decay: 5×10^{-5}
- Gradient clipping: 0.1

3.2 Manipulating the Receptive Field

There is plentiful of ways for Manipulating the receptive field. It is known that the presence of skip connections affect the receptive fields along with depth and dilation on convolutions. We wanted to alter the receptive field minimum alterations to the rest of the networks leaving all layers with the exact same number of parameters. We placed a maxpooling layer just after the first convolutional layer on both architectures and we changed the kernel size of that layer. That is the only difference between the different models on each experiment. For each architecture-dataset-receptive field combination we trained 5 models and the result are shown in 3.3.

3.3 Receptive Field, Accuracy and Pruning

Here we show the dense accuracy after training the models and its one-shot pruned accuracy. One interesting observation is that larger receptive field correlates with lower accuracy but simultaneously its one-shot pruning performances is better than those for smaller receptive fields. This behaviour generalises across all the combinations of architecture-dataset. In Section I.1 we show that the current trend in accuracy (for dense and prune version) only arises for sufficiently large pruning rate (>0.8). We also fine-tuned the models to test their real-world application capabilities as seen in Section 3.4 but here we only show the pruning rate of 0.9 as means to show the one-shot behaviour of these networks in order to understand their one-shot potential. For each one of the combinations shown here we trained and pruned 5 models, the values presented are the mean with its standard deviation.

The image size for CIFAR10 and Tiny ImageNet is 32x32 and 64x64 respectively. In both cases the receptive fields of each architecture is greater than the size of the image.

VGG Accuracy			
Receptive Field	**Dense**	**Pruned (90%)**	**Difference in Accuracy**
181	93.5 ± 0.11	10.9 ± 2.03	82.6 ± 2.02
359	91.1 ± 0.23	32.4 ± 15.7	58.7 ± 15.8
537	87.8 ± 0.19	87.6 ± 0.30	0.18 ± 0.16
715	85.8 ± 0.21	85.8 ± 0.22	0.07 ± 0.04
ResNet 50 Accuracy			
Receptive Field	**Dense**	**Pruned (90%)**	**Difference in Accuracy**
110	94.8 ± 0.29	56 ± 20.7	38.7 ± 20.5
213	94.0 ± 0.16	91.7 ± 0.98	2.25 ± 0.90
318	92.2 ± 0.18	91.4 ± 0.45	0.85 ± 0.49
423	90.4 ± 0.30	90.2 ± 0.37	0.18 ± 0.09

Table 1: **CIFAR10 results:** Here are summarised the results for the experiments performed in CIFAR10. It can be seen that the discrepancy in accuracy between different receptive fields is consistent for these two architectures. Also, as we increase the receptive field we can see that the gap in performance between dense and pruned models diminishes. The pruning rate used is 90%

VGG Accuracy			
Receptive Field	**Dense**	**Pruned**	**Difference in Accuracy**
181	61.5 ± 0.33	0.75 ± 0.09	60.8 ± 0.32
359	53.2 ± 0.20	0.63 ± 0.17	52.6 ± 0.36
537	41.0 ± 1.91	16.7 ± 7.50	24.3 ± 5.81
715	38.5 ± 1.69	21.8 ± 6.57	16.7 ± 7.21
ResNet 50 Accuracy			
Receptive Field	**Dense**	**Pruned**	**Difference in Accuracy**
213	61.8 ± 0.40	5.91 ± 0.89	55.9 ± 0.99
318	59.1 ± 0.36	8.56 ± 2.66	50.5 ± 2.55
423	56.5 ± 0.27	21.4 ± 2.87	35.0 ± 2.99

Table 2: **Tiny ImageNet Results:** Here are summarised the results for the experiments performed in Tiny ImageNet. Similarly to CIFAR10, the trend of diminishing dense accuracy and gap between dense and pruned accuracy as we increase the receptive field is consistent in the two architectures. The pruning rate is 90% excluding the first convolutional layer and the linear layer

3.4 Fine-tuning Pruned Solutions

Here we fine-tuned the pruned solutions while preserving the mask for 10 epochs with the following hyper-parameters

- Initial Learning Rate: 0.0001,
- Weight Decay:5e-4
- Momentum:0,9

- Gradient clip: 0.1

VGG Accuracy			
Receptive Field	**Dense**	**Pruned (90%)**	**Difference In Accuracy**
181	93.52±0.115	91.42±2.026	2.106±2.111
359	91.15±0.232	90.81±0.293	0.348±0.366
537	87.88±0.193	87.85±0.223	0.032±0.070
715	85.88±0.217	85.78±0.286	0.096±0.140
ResNet50 Accuracy			
Receptive Field	**Dense Test Accuracy**	**Pruned (90%)**	**Difference In Accuracy**
110	94.69±0.213	90.86±0.701	3.830±0.795
213	94.03±0.236	93.55±0.211	0.477±0.197
318	92.22±0.244	92.03±0.200	0.190±0.053
423	90.23±0.169	90.23±0.147	-0.007±0.087

Table 3: VGG and ResNet50 on CIFAR10 with fine tuning and pruning rate 0.9

VGG			
Receptive Field	**Dense Test Accuracy**	**Pruned (90%)**	**Difference In Accuracy**
181	61.58±0.333	30.21±2.595	31.37±2.534
359	53.25±0.207	3.558±2.027	49.69±2.188
537	41.05±1.917	38.21±2.699	2.842±0.884
715	38.57±1.691	36.45±1.549	2.126±0.762
ResNet50			
Receptive Field	**Dense Test Accuracy**	**Pruned (90%)**	**Difference In Accuracy**
213	61.83±0.401	44.56±1.205	17.27±1.346
318	59.10±0.368	44.28±0.648	14.82±0.633
423	56.53±0.279	46.16±0.716	10.37±0.577

Table 4: VGG and ReseNet50 on Tiny ImageNet with fine tuning and pruning rate of 0.9

Tiny ImageNet for 100 Epochs

VGG Test Accuracy			
Receptive Field	**Dense**	**Pruned (90%)**	**Difference In Accuracy**
181	61.58±0.333	33.93±0.320	27.66±0.521
359	53.25±0.207	29.73±16.15	23.52±16.23
537	41.05±1.917	37.50±1.916	3.554±0.164
715	38.57±1.691	35.50±1.812	3.078±0.453
ResNet50 Test Accuracy			
Receptive Field	**Dense**	**Pruned (90%)**	**Difference In Accuracy**
213	61.83±0.401	50.21±0.428	11.62±0.487
318	59.10±0.368	49.83±0.583	9.274±0.413
423	56.53±0.279	49.43±0.403	7.106±0.361

Table 5: VGG and ReseNet50 on Tiny ImageNet with fine tuning for 100 epochs and pruning rate of 0.9

3.5 Loss Landscape and Receptive Field

Why do models with large receptive field behave in this manner? One hypothesis is that the loss landscape changes in such a way that makes more difficult for SGD to found a better solution. In Figures 1 and 2 we show the 90 largest eigen values for both models on CIFAR10, before and after training. As we can see, at the beginning of training the Hessian spectra of models with alter receptive field are wider and encompass larger eigen values. This means that the landscape of that models has much more steeper directions of descent (and ascent) making the landscape more chaotic and difficult to traverse than for smaller receptive fields (maybe search a citation that corroborates this?).

Talk about the training trajectory in Figure 3, and mention that the figures in Figures 1 and 2 explain such behaviour. In Figure 3a I trained for double the epochs trying to show that even with more training the larger receptive field cannot match the smaller receptive field. The bump seen arround 200 epochs is due tu the learning rate schedule, which is a cosine schedule with Tmax=200, right now im training a model with Tmax=400 to see if it that claim is still valid. All the accuracies seen throughtout the document correspond to the best model while trainig e.g. the bump

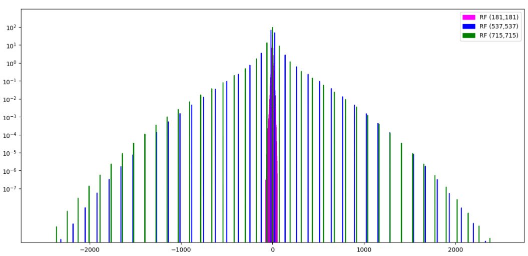

(a) Before Training

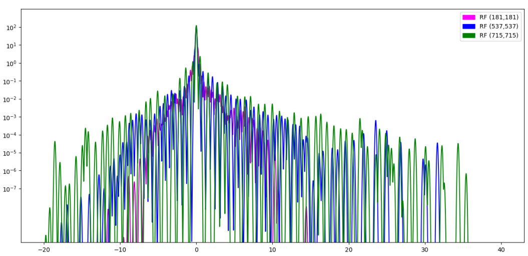

(b) After training

Figure 1: Largest 90 eigen values of VGG model on CIFAR10 for different Receptive Fields

Here I can put labels like λ and $P(\lambda)$. Larger font

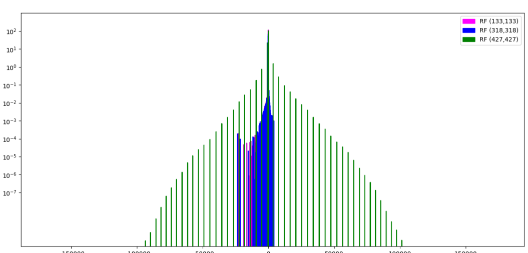

(a) Before Training

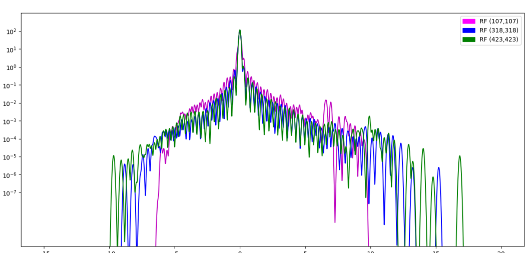

(b) After training

Figure 2: Largest 90 eigen values of ResNet50 model on CIFAR10 for different Receptive Fields

But how does this affect the features or representations that these models learn? Next we show the similarity of the internal representation two different seeds of the ReseNet50 model on CIFAR10., It is observed that the introduction of larger receptive fields results in a divergence of representations within the deepest layers. This phenomenon can be attributed to the heightened "chaotic" nature of the loss landscape, as indicated by the Hessian spectra in Figure 2, particularly in instances where larger receptive fields are employed. Notably, the representations in deeper layers for individual seeds exhibit dissimilarity, as they tend to converge into distinct basins, differing not only from the majority of the network but also from corresponding layers in other seeds. The representation similarly was calculated using the first 1000 images of the test set and we use the Centred linear Kernel Alignment [Kornblith et al., 2019] as similarity measure.

In Figure 4 we can see that the similarity between layers decreases as we increase the receptive field. This is consistent with our findings that the loss landscape for large receptive fields are more "rugged" (see Figures 1 and 2) meaning that deeper layers, which learn specific features for the

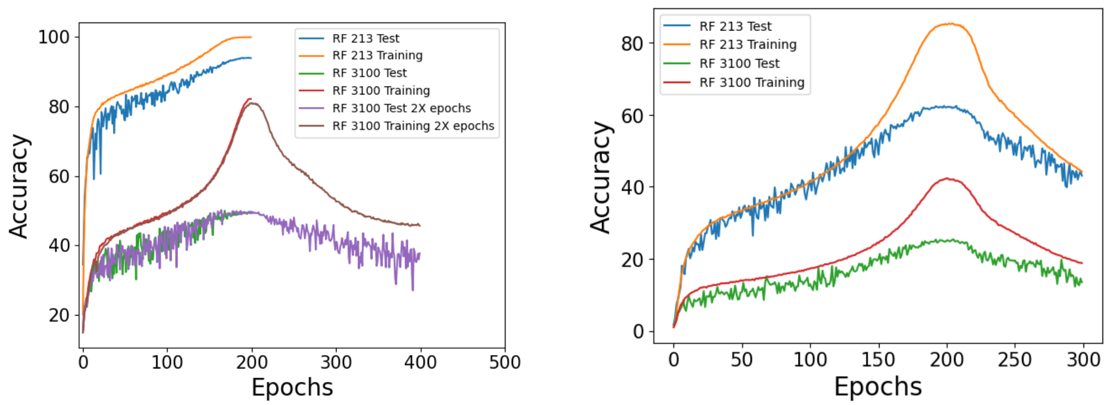

(a) ResNet50 training for different Receptive fields on CIFAR10

(b) ResNet50 training for different Receptive fields on Tiny ImageNet

Figure 3: Training of ResNet50 on CIFAR10 and Tiny ImageNet

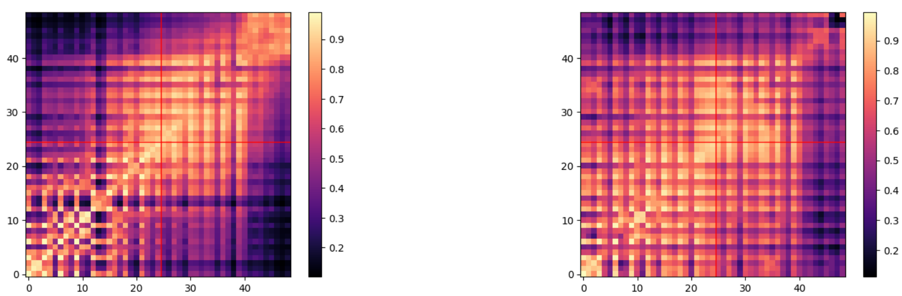

(a) Receptive Field 110

(b) Receptive Field 213

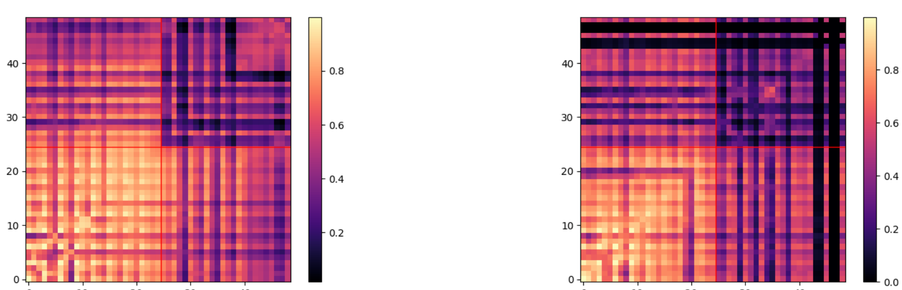

(c) Receptive Field 318

(d) Receptive Field 423

Figure 4: Representation similarly for all convolutional layers in ReseNet50 for different receptive fields. The red lines represent the middle layer of the model (25^{th} layer). The largest receptive field (bottom right) has high degree of dissimilarity between its deeper layer representations when compared with the smallest receptive field (top left)

task [Ro and Choi, 2021; Yosinski et al., 2014], converge to a more varied set of representations thus the increase in dissimilarity. The shallow layers in the other hand, converge to a more uniform set of representations, hence their similarity. This is congruent with the notion that shallow layer learn "general " features that subsequent layers build more specific/complex features. [Ro and Choi, 2021]. Conversely, smaller receptive fields have a smoother loss landscape and in consequence, even the deeper, specific layers in the network converge to similar representations. Another explanation is that due to the size of the receptive field, the network's ability to learn nuanced features (those that normally would be learned in deeper layers) is impaired, thus affecting its performance and similarities.

3.6 Large Receptive Field for Tiny ImageNet

ResNet50 Test Accuracy			
Receptive Field	**Dense**	**Pruned (90% One Shot)**	**Difference In Accuracy**
1415	32.00±0.192	32.00±0.192	0.000±0.000
1920	29.28±0.627	29.28±0.627	0.000±0.000
3100	22.84±0.370	22.84±0.370	0.000±0.000

Table 6: ReseNet50 with large Receptive Field on Tiny ImageNet with pruning rate of 0.9

3.7 Large Receptive Field for CIFAR10

ResNet50 Accuracy			
Receptive Field	**Dense**	**Pruned (90% One Shot)**	**Difference in Accuracy**
1415	72.87±0.787	72.87±0.787	0.000±0.000
1920	53.37±1.293	53.37±1.293	0.000±0.000
3100	50.11±0.256	50.11±0.256	0.000±0.000

Table 7: ReseNet50 with large receptive field in CIFAR10

3.8 Width and Depth can partially Recover Information

One question is : Is the information from the receptive field not recoverable by the width or depth of the model? To answer this, we modified the width of ResNet50 by 2x and 3x times and found that despite the marginal improvement in performance, the width of the model cannot retrieve all the information lost by the large receptive field, thus diverging from the observation that accurate information can be extracted by coarsely tuned units [Ballard et al., 1983].

Receptive Field	**Width**		
	$\times$**1**	$\times$**2**	$\times$**3**
318	59.10±0.368	60.97	**Pending**
1415	32.00±0.192	37.36	38.0
3100	22.84±0.370	26.33	26.04

Table 8: Accuracies for ResNet50 Model on Tiny ImageNet for different woitdhs, We can see here that withd can only recover information on very large receptive fields. This means that for a small receptive field all information necessary for the task is included is available to the network.

Here I'm planning to include results of a ResNet24 model that has all the same components as ReseNet50 but it simply is more shallow. Also, I am running experiments on width for two more receptive fields, 318 and 1415. Also, I have not implemented / shown the information measure we talked about with Netta, but, as Netta suggested, it can simply be $\frac{\text{Difference in Accuracy}}{\text{Dense Accuracy}}$

4 Conclusions and Future work

In this work, we showed how the receptive field affects the loss landscape of neural networks along with its representations and its behaviour on the input image. It is important to note that there are other ways to manipulate the receptive field such as changing the kernel size of the convolutional networks,stride, and dilation of the convolutional networks. In this work, used the minimum intervention that would not modify the number of weights of the models as we manipulated the receptive field of the models. Additionally, as we changed the receptive field of the models we changed the size of internal representations, which can greatly affect the behaviour of the models. Future work will concentrate on testing other ways to manipulate the receptive field, such as dilation of the maxpooling layer, in addition to using padding to maintain constant the size of internal representations across receptive fields to test the robustness of the findings in this work.

References

D. H. Ballard, G. E. Hinton, and T. J. Sejnowski. Parallel visual computation. *Nature*, 306(5938): 21–26, Nov. 1983. ISSN 1476-4687. doi: 10.1038/306021a0.

J. Deng, W. Dong, R. Socher, L.-J. Li, K. Li, and L. Fei-Fei. ImageNet: A large-scale hierarchical image database. In *2009 IEEE Conference on Computer Vision and Pattern Recognition*, pages 248–255, June 2009. doi: 10.1109/CVPR.2009.5206848.

J. Devlin, M.-W. Chang, K. Lee, and K. Toutanova. BERT: Pre-training of Deep Bidirectional Transformers for Language Understanding. In *Proceedings of the 2019 Conference of the North American Chapter of the Association for Computational Linguistics: Human Language Technologies, Volume 1 (Long and Short Papers)*, pages 4171–4186, Minneapolis, Minnesota, June 2019. Association for Computational Linguistics. doi: 10.18653/v1/N19-1423.

I. Goodfellow, Y. Bengio, and A. Courville. *Deep Learning*. MIT Press, 2016.

B. J. Kim, H. Choi, H. Jang, D. G. Lee, W. Jeong, and S. W. Kim. Dead pixel test using effective receptive field. *Pattern Recognition Letters*, 167:149–156, Mar. 2023. ISSN 0167-8655. doi: 10.1016/j.patrec.2023.02.018.

G. Kobayashi and H. Shouno. Interpretation of ResNet by Visualization of Preferred Stimulus in Receptive Fields, July 2020.

S. Kornblith, M. Norouzi, H. Lee, and G. Hinton. Similarity of Neural Network Representations Revisited, July 2019.

Y. LeCun, Y. Bengio, and G. Hinton. Deep learning. *nature*, 521(7553):436–444, 2015.

W. Luo, Y. Li, R. Urtasun, and R. Zemel. Understanding the Effective Receptive Field in Deep Convolutional Neural Networks. In *Advances in Neural Information Processing Systems*, volume 29. Curran Associates, Inc., 2016.

Y. Ro and J. Y. Choi. AutoLR: Layer-wise pruning and auto-tuning of learning rates in fine-tuning of deep networks. In *Proceedings of the AAAI Conference on Artificial Intelligence*, volume 35, pages 2486–2494, 2021.

A. van den Oord, S. Dieleman, H. Zen, K. Simonyan, O. Vinyals, A. Graves, N. Kalchbrenner, A. Senior, and K. Kavukcuoglu. WaveNet: A Generative Model for Raw Audio. *arXiv:1609.03499 [cs]*, Sept. 2016.

J. Yosinski, J. Clune, Y. Bengio, and H. Lipson. How transferable are features in deep neural networks? In *Advances in Neural Information Processing Systems*, volume 27. Curran Associates, Inc., 2014.

B. Zhou, A. Khosla, A. Lapedriza, A. Oliva, and A. Torralba. Object Detectors Emerge in Deep Scene CNNs, Apr. 2015.

I Supplementary Material

Model Implementation details

Here are the implementation details.

I.1 One-shot Solutions with Multiple Pruning Rates

For every combination 5 models were trained, pruned and fine-tuned. The error bars correspond to the standard deviation.

Pruning Rate 0.8

VGG Accuracy			
Receptive Field	**Dense**	**Pruned**	**Difference In Accuracy**
181	93.52±0.115	72.22±27.11	21.30±27.18
359	91.15±0.232	90.23±1.32	0.916±1.50
537	87.87±0.193	87.87±0.193	0.0\pm$0.0
715	85.88±0.217	85.880±0.217	0.0±0.0
ResNet50			
Receptive Field	**Dense**	**Pruned**	**Difference In Accuracy**
110	94.69±0.213	92.34±1.084	2.350±0.921
213	94.03±0.236	93.81±0.218	0.220±0.234
318	92.22±0.244	92.14±0.227	0.080±0.036
423	90.23±0.169	90.23±0.145	-0.003±0.035

Table S1: VGG and ResNet50 on CIFAR10 and pruning rate 0.8

VGG Accuracy			
Receptive Field	**Dense**	**Pruned**	**Difference In Accuracy**
181	61.58±0.333	19.14±4.610	42.44±4.669
359	53.25±0.207	10.09±1.931	43.16±2.085
537	41.05±1.917	40.09±2.129	0.958±0.360
715	38.57±1.691	37.87±1.566	0.700±0.524
ResNet50 Accuracy			
Receptive Field	**Dense**	**Pruned**	**Difference In Accuracy**
213	61.83±0.401	40.56±3.039	21.27±3.170
318	59.10±0.368	43.09±1.880	16.01±1.824
423	56.53±0.279	49.27±0.580	7.260±0.412

Table S2: VGG and ResNet50 Tiny ImageNet pruning rate 0.8

Pruning Rate 0.7

VGG Accuracy			
Receptive Field	**Dense**	**Pruned**	**Difference In Accuracy**
181	93.52±0.115	93.32±0.104	0.206±0.155
359	91.15±0.232	91.10±0.230	0.058±0.050
537	87.88±0.193	87.88±0.193	0.0±0.0
715	85.88±0.217	85.88±0.217	0.0±0.0
ResNet50 Accuracy			
Receptive Field	**Dense**	**Pruned**	**Difference In Accuracy**
110	94.69±0.213	94.24±0.204	0.453±0.012
213	94.03±0.236	93.93±0.203	0.097±0.093
318	92.22±0.244	92.24±0.254	-0.020±0.010
423	90.23±0.169	90.23±0.175	-0.007±0.006

Table S3: VGG and ResNet50 on CIFAR10 and pruning rate 0.7

VGG			
Receptive Field	**Dense**	**Pruned**	**Difference In Accuracy**
181	61.58±0.333	48.29±1.390	13.29±1.462
359	53.25±0.207	40.02±2.558	13.23±2.646
537	41.05±1.917	40.96±1.934	0.092±0.070
715	38.57±1.691	38.51±1.658	0.068±0.087
ResNet50			
Receptive Field	**Dense**	**Pruned**	**Difference In Accuracy**
213	61.83±0.401	55.33±0.987	6.504±1.194
318	59.10±0.368	54.28±0.398	4.816±0.319
423	56.53±0.279	54.41±0.449	2.128±0.216

Table S4: VGG and ResNet50 on Tiny ImageNet and pruning rate 0.7

Pruning Rate 0.6

VGG Accuracy			
Receptive Field	**Dense**	**Pruned**	**Difference In Accuracy**
181	93.52±0.115	93.48±0.109	0.048±0.050
359	91.15±0.232	91.15±0.240	0.004±0.015
537	87.88±0.193	87.88±0.193	0.000±0.000
715	85.88±0.217	85.88±0.217	0.000±0.000
ResNet50 Accuracy			
Receptive Field	**Dense**	**Pruned**	**Difference In Accuracy**
110	94.69±0.213	94.61±0.190	0.080±0.026
213	94.03±0.236	94.01±0.234	0.020±0.020
318	92.22±0.244	92.23±0.225	-0.010±0.020
423	90.23±0.169	90.23±0.169	0.000±0.000

Table S5: VGG and ResNet50 CIFAR10 pruning rate 0.6

VGG Accuracy			
Receptive Field	**Dense**	**Pruned**	**Difference In Accuracy**
181	61.58±0.333	56.93±0.512	4.656±0.663
359	53.25±0.207	47.94±1.896	5.304±1.963
537	41.05±1.917	41.05±1.913	-0.000±0.071
715	38.57±1.691	38.58±1.659	-0.008±0.039
ResNet50 Accuracy			
Receptive Field	**Dense**	**Pruned**	**Difference In Accuracy**
213	61.83±0.401	59.28±0.468	2.552±0.489
318	59.10±0.368	57.26±0.467	1.840±0.356
423	56.53±0.279	55.97±0.459	0.568±0.212

Table S6: VGG and ResNet50 Tiny ImageNet pruning rate 0.6

Pruning Rate 0.5

VGG Accuracy			
Receptive Field	**Dense**	**Pruned**	**Difference In Accuracy**
181	93.52±0.115	93.51±0.128	0.010±0.029
359	91.15±0.232	91.16±0.237	-0.004±0.005
537	87.88±0.193	87.88±0.193	0.000±0.000
715	85.88±0.217	85.88±0.217	0.000±0.000
ResNet50 Accuracy			
Receptive Field	**Dense**	**Pruned**	**Difference In Accuracy**
110	94.69±0.213	94.71±0.202	-0.023±0.012
213	94.03±0.236	94.02±0.243	0.010±0.026
318	92.22±0.244	92.22±0.229	-0.003±0.015
423	90.23±0.169	90.23±0.169	0.000±0.000

Table S7: VGG and ResNet50 on CIFAR10 with pruning rate 0.5

VGG Accuracy			
Receptive Field	**Dense**	**Pruned**	**Difference In Accuracy**
181	61.58±0.333	59.85±0.241	1.738±0.240
359	53.25±0.207	51.13±0.665	2.116±0.735
537	41.05±1.917	41.05±1.915	-0.004±0.018
715	38.57±1.691	38.57±1.686	0.008±0.013
ResNet50 Accuracy			
Receptive Field	**Dense**	**Pruned**	**Difference In Accuracy**
213	61.83±0.401	60.86±0.458	0.966±0.400
318	59.10±0.368	58.46±0.510	0.640±0.401
423	56.53±0.279	56.29±0.408	0.248±0.180

Table S8: VGG and ResNet50 Tiny ImageNet with pruning rate 0.5